Original Research

Uniform neural tissue models produced on synthetic hydrogels using standard culture techniques

Christopher Barry[1], Matthew T Schmitz[1], Nicholas E Propson[1], Zhonggang Hou[1,2], Jue Zhang[1], Bao K Nguyen[1], Jennifer M Bolin[1], Peng Jiang[1], Brian E McIntosh[1], Mitchell D Probasco[1], Scott Swanson[1], Ron Stewart[1], James A Thomson[1,3,4], Michael P Schwartz[5] and William L Murphy[6,7,8]

[1]Morgridge Institute for Research, Madison, WI 53705, USA; [2]Department of Biological Chemistry, University of Michigan Medical School, Ann Arbor, MI 48109, USA (current address); [3]Department of Cell & Regenerative Biology, University of Wisconsin-Madison, Madison, WI 53705, USA; [4]Department of Molecular, Cellular, & Developmental Biology, University of California, Santa Barbara, CA 93106, USA; [5]Center for Sustainable Nanotechnology, Department of Chemistry, University of Wisconsin-Madison, Madison, WI 53706, USA; [6]Department of Biomedical Engineering, University of Wisconsin-Madison, Madison, WI 53705, USA; [7]Materials Science Program, University of Wisconsin-Madison, WI 53705, USA; [8]Department of Orthopedics and Rehabilitation, University of Wisconsin-Madison, Madison, WI 53705, USA

The first two authors contributed equally to this paper.

Corresponding authors: William L Murphy. Email: wlmurphy@wisc.edu; Michael P Schwartz. Email: mpschwartz@wisc.edu

Impact statement

Pluripotent stem (PS) cells have been characterized by an inherent ability to self-organize into 3D ''organoids'' resembling stomach, intestine, liver, kidney, and brain tissues, offering a potentially powerful tool for modeling human development and disease. However, organoid formation must be quantitatively reproducible for applications such as drug and toxicity screening. Here, we report a strategy to produce uniform neural tissue constructs with reproducible global gene expression profiles for replicate samples from multiple experiments.

Abstract

The aim of the present study was to test sample reproducibility for model neural tissues formed on synthetic hydrogels. Human embryonic stem (ES) cell-derived precursor cells were cultured on synthetic poly(ethylene glycol) (PEG) hydrogels to promote differentiation and self-organization into model neural tissue constructs. Neural progenitor, vascular, and microglial precursor cells were combined on PEG hydrogels to mimic developmental timing, which produced multicomponent neural constructs with 3D neuronal and glial organization, organized vascular networks, and microglia with ramified morphologies. Spearman's rank correlation analysis of global gene expression profiles and a comparison of coefficient of variation for expressed genes demonstrated that replicate neural constructs were highly uniform to at least day 21 for samples from independent experiments. We also demonstrate that model neural tissues formed on PEG hydrogels using a simplified neural differentiation protocol correlated more strongly to in vivo brain development than samples cultured on tissue culture polystyrene surfaces alone. These results provide a proof-of-concept demonstration that 3D cellular models that mimic aspects of human brain development can be produced from human pluripotent stem cells with high sample uniformity between experiments by using standard culture techniques, cryopreserved cell stocks, and a synthetic extracellular matrix.

Keywords: Biomaterial, development, neurotoxicology, matrix, organoid, screening

***Experimental Biology and Medicine* 2017; 242: 1679–1689. DOI: 10.1177/1535370217715028**

Introduction

Pluripotent stem (PS) cells have been characterized by an inherent ability to self-organize into 3D ''organoids'' resembling stomach[1], intestine[2], liver[3], kidney[4], and brain[5–8] tissues, offering a potentially powerful tool for modeling human development and disease,[9] and for emerging toxicity screening approaches.[10] The value of 3D cellular models will continue to expand as new strategies for inducing specialization evolve, but variability between samples has been a limitation for most organoid formation protocols to date.[11,12] Typical organoid protocols rely on media or scaffolds that include Matrigel and specialized culture techniques such as embryoid body formation to promote differentiation and self-organization, each of which likely plays a role in poor sample reproducibility. Matrigel is a poorly defined mixture of bioactive components known

to influence stem cell function,[13] while extraction from mouse Engelbreth-Holm-Swarm (EHS) tumors[14,15] is an inherent source of variability between lots, factors that are especially problematic for organoid protocols that require multiple steps and long culture times. The use of Matrigel as a scaffold is also technically challenging for applications that require automation or scale-up, since monomer solutions must be kept at low temperature to prevent premature gelation. Therefore, organoid protocols would benefit from strategies to replace Matrigel with defined matrices.

Several reports have demonstrated that PEG hydrogels and other chemically defined scaffolds are suitable for producing model 3D neural tissues or organoids,[16–19] which demonstrates that appropriate design strategies using defined scaffold materials offer an alternative to Matrigel. Thiol-ene photopolymerization provides a robust and modular chemistry for fabricating hydrogels with bioactive components such as peptides, hyaluronic acid, and gelatin.[18,20–28] In contrast to the thousands of bioactive molecules found in Matrigel,[29] poly(ethylene glycol) (PEG) hydrogels formed using thiol-ene chemistry have proven remarkably versatile as a cell culture scaffold by incorporating synthetic peptides[20,28] such as proteolytically degradable peptide crosslinks[30] and cellular adhesion peptides.[31,32] Such peptide-functionalized PEG hydrogels provide a minimum complexity, fully synthetic culture scaffold that can be tuned to control 3D cellular remodeling through matrix degradation, migration, and ECM deposition.[20,33,34] Several recent studies have demonstrated that synthetic hydrogels formed using thiol-ene chemistry are promising for neural tissue modeling approaches, including neurotoxicity screening,[18] potency testing,[22] directed differentiation,[23] and neural cell culture.[21,24]

We previously reported a strategy for producing model neural tissue constructs with 3D organization and demonstrated the value of this approach for enhanced throughput neurotoxicity screening.[18] The protocol was developed based on the notion that reproducible model neural tissues with multiple cellular components (neural, glial, vascular, and immune cells) could be produced by (1) differentiating human pluripotent stem cells into precursor populations representing major compartments of the developing human brain, (2) cryopreserving the precursor cells where possible to ensure uniform cell populations between experiments, (3) using standard culture techniques for cell handling, and (4) culturing the cells on bioactive synthetic hydrogels permissive towards cellular remodeling rather than Matrigel.[18,35] Here, we aimed to demonstrate the value of this protocol for producing uniform neural constructs by quantitatively analyzing global gene expression profiles for replicate samples from multiple experiments and by evaluating the generality of our approach using human pluripotent stem cells differentiated by a second neural induction procedure.

Materials and methods

Cell culture

DF3S medium: DMEM/F-12, L-ascorbic acid-2-phosphate magnesium (64 mg/L), sodium selenium (14 μg/L), and $NaHCO_3$ (543 mg/L). *E8 medium*[36]: DMEM/F12, L-ascorbic acid-2-phosphate magnesium (64 mg/L), sodium selenium (14 μg/L), FGF2 (100 μg/L), insulin (20 mg/L), $NaHCO_3$ (543 mg/L), transferrin (10.7 mg/L), and TGFβ1 (2 μg/L). *E7V medium*: E8 minus TGFβ1, but supplemented with 50 μg/L VEGF-A. *Mesenchymal serum-free expansion medium (M-SFEM)*: 50% StemLine II serum-free HSC expansion medium (HSFEM; Sigma-Aldrich), 50% human endothelial serum-free medium (ESFM; Invitrogen), GlutaMAX (1/100 dilution; Invitrogen), Ex-Cyte supplement (1/2000 dilution; Millipore), 100 mM monothioglycerol (MTG), and 10 μg/L rhFGF2. *Neural growth medium (NGM)*: DF3S medium supplemented with rhFGF2 (5 μg/L), 1X N2 (Life Technologies, 17502-048) and 1X B27 (Life Technologies, 17504-044) supplements. *NB+NOG neural differentiation medium:* DF3S supplemented with 1X N2, 1X B27, and 100 ng/mL recombinant human NOGGIN (R&D Systems).

''Multicomponent'' neural constructs were formed using neural progenitor cells (NPCs), endothelial cells (ECs), mural cells (mesenchymal stem cells, MSCs, or primary human pericytes, PCs), and microglia precursors (MG) that were differentiated and expanded as previously described, without modification.[18] Briefly, NPCs were differentiated as previously described and expanded using neural growth medium. Human brain vascular pericytes (ScienCell) were expanded by culturing according to manufacturer's instructions in Pericyte Medium (Catalog #1201, ScienCell). ECs were expanded on fibronectin-coated plates with E7V medium. MSCs were expanded in either M-SFEM or Pericyte medium (ScienCell, the expansion medium did not lead to measurable differences in neural tissue construct properties). Microglia precursor cells (or microglia/macrophage precursors) were freshly differentiated as previously described, without modification.[18]

''Single-component'' neural constructs were formed using H1 ES cells differentiated using a neural induction protocol that was previously described.[37] H1 ES cells were split onto Matrigel-coated plates at ~20–40% confluency in NB+NOG medium. Cells were split every 3–6 days for 14 days to prevent over confluency.

Hydrogel preparation via thiol-ene photopolymerization

Protease-degradable synthetic PEG hydrogels were fabricated as previously described in detail, without modification.[18] PEG hydrogels were formed by crosslinking 8-arm PEG-norbornene molecules (20,000 MW, JenKem USA, 8ARM (TP)-NB-20 K) with matrix metalloproteinase (MMP)-degradable peptide (GenScript, KCG**GPQGIWGQ**GCK, active sequence in bold),[30] and incorporated pendant C**RGDS** (GenScript) peptide[32] for cell adhesion. Monomer solutions were prepared at a final concentration of 40 mg/mL 8-arm PEG-NB (16 mM norbornene arms), 4.8 mM MMP-degradable peptide (9.6 mM cysteines, 60% molar ratio of cysteines to norbornene groups), 2 mM CRGDS, and 0.05% (wt/wt) photoinitiator (Irgacure 2959, or I2959) in PBS.

Multicomponent neural constructs. For most experiments using multicomponent neural constructs, hydrogels were formed by pipetting 30 μL of monomer into Corning 24-well Falcon Cell Culture Inserts (Fisher

Catalog No. 08-771-9, polyethylene terephthalate membrane, 0.3 cm^2 culture area, 1.0 μm pore size). For immunofluorescence imaging shown in Figure 3, hydrogels were formed by pipetting 40 μL of monomer into Corning HTS Transwell-24 well permeable supports (Fisher, Catalog No. 07-200-537, polyester membrane, 0.33 cm^2 culture area, 0.4 μm pore size).

Single-component neural constructs. For experiments that used the second NPC differentiation protocol,[37] some hydrogels were formed using a non-degradable PEG-dithiol crosslinker (also 60% crosslinking density) for comparison to MMP-degradable hydrogels. Hydrogels were formed by pipetting 9 μL of monomer into TPP round bottom (U-base) 96-well plates (TPP 92097). The round bottom (or U-base) geometry was chosen to minimize meniscus formation and hydrogel buckling during swelling.

Monomers were polymerized by 2.5 min of exposure to ~365 nm centered UV light (UVP XX-15 L lamp, top shelf of a UVP XX-15 lamp stand, Fisher Scientific) for all multiwell formats. The hydrogels were incubated overnight (5% CO_2, 37°C) in DF3S medium to remove excess unreacted monomer and to allow swelling and equilibration. After overnight incubation, DF3S medium was removed and cells were seeded on top of the hydrogels in neural growth medium.

Formation of neural tissue constructs

Multicomponent neural tissue constructs[18]. NPCs were seeded at a density of 50,000–150,000 cells/well, allowed to attach overnight, and then cultured in neural growth medium with a medium exchange on day 1 and every two days thereafter. At day 9, ECs and MSCs or primary pericytes were seeded 5:1 (ECs:MSCs or ECs:PCs) in neural growth medium at a total density of 100,000 cells per well. Neural growth medium was exchanged on day 11 (2 days after seeding ECs and MSCs/PCs). Microglia precursors were seeded in neural growth medium at a density of 25,000 cells per insert on day 13. Neural growth medium was then exchanged on day 14 and every two days thereafter.

Single-component neural constructs[37]. NPCs were seeded at a density of 100,000 or 200,000 cells/well of round bottom 96-well plates, allowed to attach overnight, and then cultured in neural growth medium with a medium exchange on day 1 and every two days thereafter. At day 7 of growth on MMP-degradable or non-degradable PEG hydrogels (day 21 total), neural growth medium was switched to the base DF3S medium without additional neural supplements or growth factors for one set of samples (labeled DF3S).

Immunofluorescence imaging

Primary antibodies. Mouse anti-CD31 (Dako, M082301-2, 1:200 dilution), Rabbit anti-Glial Fibrillary Acidic Protein (GFAP, DAKO Z033401-2, 1:500), Rabbit anti-β3-Tubulin (Cell Signaling, 5568S, 1:500), Mouse β3-Tubulin (R&D Systems, MAB1195, 1:500), Goat Iba1 (AIF1, Abcam ab5076, 1:100).

Secondary antibodies. Donkey anti-Rabbit 488 (Life Technologies, A21206, 1:200), Donkey anti-Mouse 488 (Life Technologies, A21202, 1:200), Donkey anti-Goat 568 (Life Technologies, A11057, 1:200), Donkey anti-Rabbit 568 (Life Technologies, A10042, 1:200), Donkey anti-Mouse 647 (Life Technologies, A31571, 1:200). Neural constructs were fixed for 60 min in 2% buffered formalin and stored in PBS at 4°C until further processing, and all steps were conducted within the transwell insert. Neural constructs were permeabilized and blocked in blocking buffer (0.25% Triton X-100 and 1% BSA) in PBS for at least 60 min. Primary antibodies in incubation buffer (0.05% Triton X-100 and 1% BSA in PBS) were added to the transwell insert and incubated overnight at 4°C, rinsed 2 × 60 min with rinse buffer (0.05% Triton X-100 in PBS), and at least 60 min in blocking buffer. Secondary antibodies and 5 μg/mL DAPI (MP Biomedicals, 157574) in incubation buffer were added to the neural constructs, incubated overnight at 4°C or at least 4 h at room temperature, rinsed 2 × 60 min and a third time overnight at 4°C in rinse buffer, and stored in PBS (at least 24 h) until further processing. Neural constructs were removed from the transwell membrane and mounted in Aqua Polymount solution (Polysciences, Inc.) on the bottom of a 35-mm glass bottom dish (MatTek) with a coverslip over the top and then imaged on a Nikon A1R laser scanning confocal microscope and processed using NIS Elements or ImageJ.[38] Some images were adjusted using the auto correction feature for brightness/contrast in Image J and any changes were applied to the entire image as displayed.

RNA-Seq

Neural constructs were lysed in the insert by adding 350 μL RLT lysis buffer (Qiagen), and total RNA was isolated using Qiagen's RNeasy 96 kit beginning with step 3 of the manufacturer's protocol (RNeasy 96 Handbook 01/2002, using Spin Technology and the optional DNase treatment). Multicomponent neural constructs (Supplementary Tables 1 and 2)[18] were prepared for RNA-Seq with Illumina's TruSeq RNA sample preparation Kit v2 following the low-throughput (LT) protocol (TruSeq RNA Sample Preparation Guide, Part # 15008136, Rev. A). At day 35, single-component neural constructs (Supplementary Tables 2 and 3)[37] were prepared using the Ligation-Mediated Sequencing (LMSeq) protocol.[35] The cDNA libraries were pooled and run on Illumina's HiSeq 2500.

RNA-Seq data analysis. Raw reads were downloaded from the Gene Expression Omnibus[39,40] for the NPC time course on TCP (GEO accession number: GSE90053),[37] CORTECON (GEO accession number: GSE56796),[41] and cerebral organoid (GEO accession number: GSE80264)[42] datasets. FASTQ files were generated by CASAVA (v1.8.2) and Bowtie (v0.12.8)[43] was used to map reads to the human transcriptome (RefGene v1.2.3).[44] RSEM (v1.2.3)[44] was used to calculate expected counts and normalized gene

expression values, which are expressed as Transcript per Million (TPM) Reads. Coefficient of variation (CV = S.D. TPM/Mean TPM) was determined for all genes with mean TPM ≥ 1 for the sample set being analyzed. HDBR RNA-seq count values were obtained from the EMBL-EBI Gene Expression Atlas (dataset id: E-MTAB-4840).[45]

Differential gene expression. For select comparisons between datasets, gene ontology (GO) terms from the DAVID Bioinformatics Database (Resources version 6.7) Functional Annotation Tool[40,46,47] were used to identify functional properties for two-fold differentially expressed genes with $p < 0.005$ or $p < 0.001$ (Student's *t*-test).

Previous datasets were used in this study

RNA-Seq data that were previously deposited on the Gene Expression Omnibus[39,40] were used in the present study. Datasets that were analyzed from previous studies included multicomponent neural constructs (NPC-EC-MSC ± MG, Day 21, Supplementary Table 1, Supplementary Table 4, Supplementary Figure 2) and quadruplicate H1 ES cell samples (Supplementary Table 3) (GEO Series accession number GSE63935),[18] the neural differentiation time course on TCP (GEO Series accession number GSE90053)[37] that was compared to single-component neural constructs here (Figure 5, Supplementary Figures 1 and 2), CORTECON samples (GEO Series accession number GSE56796),[41] and cerebral organoids (GEO Series accession number GSE80264)[42] (Supplementary Figure 2).

Results and discussion

The developing brain is comprised of cellular compartments with distinct embryologic origins, including neurons and glial cells,[48–52] a vasculature,[53,54] and specialized immune cells (microglia).[55–57] Procedures for producing organoids with neuronal populations that resemble one or more distinct brain regions have been reported,[5–8,58] but common media formulations that are used for these protocols do not allow the same starting population of pluripotent stem cells to be differentiated down neuronal, vascular, and microglial lineages simultaneously. We previously reported a protocol to incorporate distinct components of the developing brain into a model neural tissue by combining precursors cells derived from the H1 human embryonic stem cell line (H1 ES cells) for each lineage on the same scaffold (Figure 1(a)), including neural progenitor cells (NPCs, precursors for neurons and glia), ECs, mural cells (MSCs), and microglia precursor cells.[18] For the present study, we also used primary human brain vascular pericytes as the mural component instead of MSCs for some experiments. Organoid culture techniques typically require one or more steps where pluripotent stem cells are aggregated or encapsulated within Matrigel scaffolds (or both),[58] each of which likely contributes variability that has limited sample reproducibility for previous protocols. Importantly, our protocol was optimized using standard culture techniques to seed single cell suspensions of precursor cells on synthetic PEG hydrogels (see Materials and methods for details),[18] rather than more complex procedures such as embryoid body formation or encapsulation within a matrix. Precursor cells were expanded, singularized, and cryopreserved to provide a well-defined starting population when producing model neural tissues for replicate experiments, with the exception of microglia, which were freshly differentiated.

The timing for adding precursor cells to PEG hydrogels was chosen based on the approximate sequence observed during brain development (Figure 1(a)). Since capillaries penetrate the developing human brain after the neural tube has formed,[53,54] ECs and mural cells (either MSCs or primary pericytes) were added after initial differentiation and multilayer formation by NPCs. By day 12, vascular networks were aligned with $GFAP^+$ radial glial cells, and some $GFAP^+$ cells appeared to form connections through end feet[54] (Figure 1(b) and (d), see arrows). Microglia are sparsely distributed in the early neural tube, but increase in abundance with timing that overlaps with early capillary formation.[57] Therefore, microglia precursors were added on day 13 (Figure 1(a)), by which time vascular networks were evident within the neural constructs (Figure 1(b) to (d)). Immunofluorescence imaging identified $IBA1^+$ microglia by day 14 (Figure 2(a)), and RNA-seq demonstrated that microglial genes (*AIF1*/*IBA1*, *TREM2*, *CD14*, and others) were upregulated over control samples without microglia (Figure 2(b), Supplementary Table 1). Further, GO analysis[40,46,47] demonstrated that ≥2-fold upregulated ($p < 0.005$) genes for neural constructs with microglia were predominantly associated with immune cell function when compared to samples without microglia (Figure 2(c), Supplementary Table 1). By day 21, neural constructs were characterized by multilayered neuronal organization that was particularly pronounced at the outer edges of the tissues (Figure 3(a) to (c)), and similar morphological features were observed on a millimeter scale for replicate samples (Figure 3(c) and (d); see white dashed lines tracing nuclei in the central region of the samples).

RNA-seq and Spearman's rank correlation analyses were used to compare reproducibility between replicate neural constructs formed under a variety of conditions (Supplementary Table 4). First, sample uniformity was compared for day 14 or day 21 neural constructs formed under the following conditions within the same experiment: (1) An initial seeding density of 50,000 or 100,000 NPCs per well, (2) MSCs or pericytes as the mural component, and (3) either with or without microglia (NPCs seeded alone on day 21 were also included as a control). A comparison of Spearman's coefficients (ρ) for replicate neural constructs from the same experiment were highly uniform for each set of conditions analyzed ($\rho = 0.99$ for all replicate comparisons, Supplementary Table 4), including six separate sets of quadruplicate samples that were formed with MSCs as the mural component (Figure 2(d), Supplementary Table 4: 50,000 and 100,000 NPCs per well, with or without microglia, days 14 and 21). Replicate samples from two independent experiments were also highly correlated at day 14 ($\rho \geq 0.98$; $N = 6$ replicate samples; two samples for experiment #1, four samples from two separate cryopreserved vials of NPCs for experiment #2) and day 21 ($\rho = 0.99$,

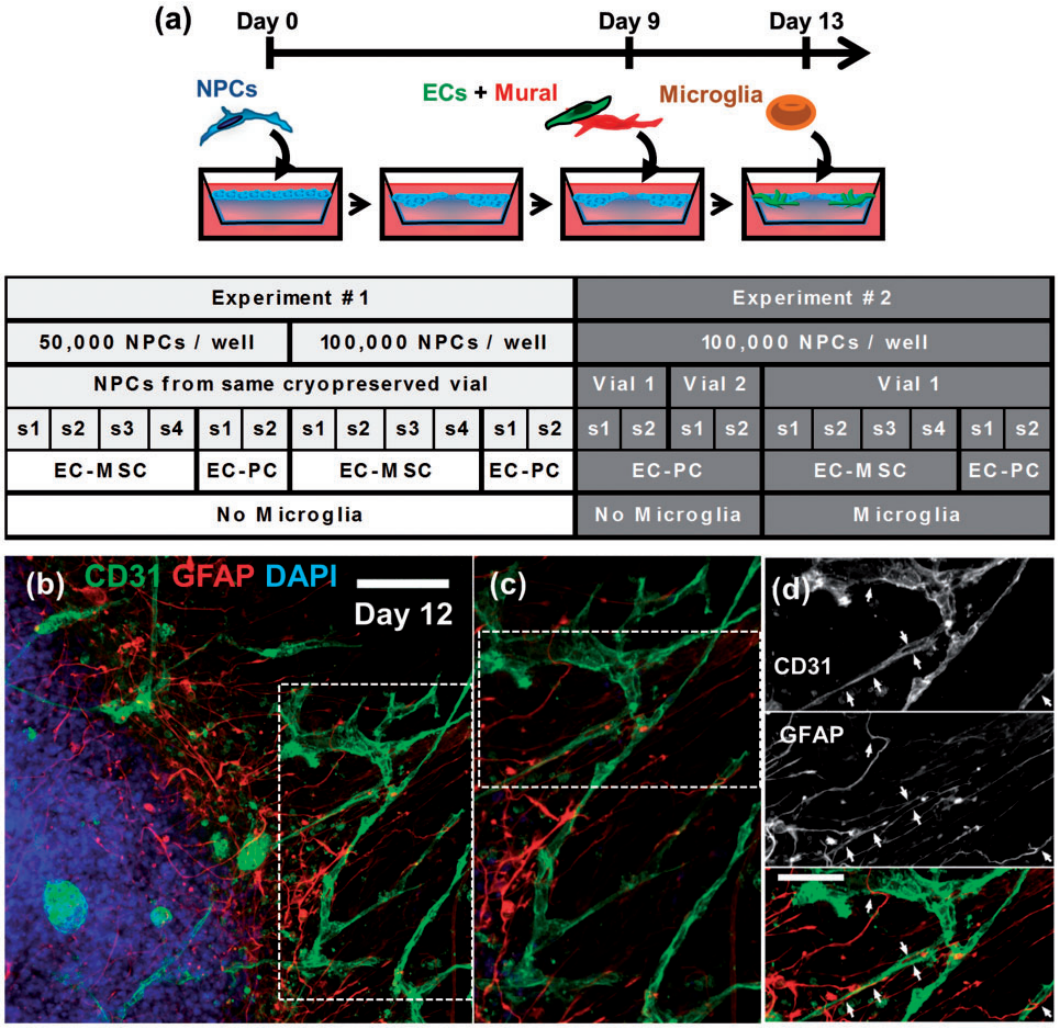

Figure 1 Procedure for producing multicomponent neural constructs. (a) Neural tissue constructs (also referred to as ''multicomponent'' neural constructs) were formed by combining H1 ES cell-derived neural progenitor cells (NPCs), endothelial cells (ECs), and mesenchymal stem cells (MSCs) from cryopreserved stocks. Primary human brain-derived pericytes (PCs) from cryopreserved stocks were used instead of MSCs and freshly differentiated microglia precursor cells were added on day 13 where indicated. Precursors were cultured on top of peptide-functionalized polyl(ethylene glycol) (PEG) hydrogels in 24-well Transwell inserts. Table: Overview of replicate multicellular neural constructs analyzed in this study. Samples formed with pericytes and without microglia were prepared using two separate cryopreserved vials of NPCs for experiment #2. Replicate samples for a given condition are labeled by sample number (e.g. sample 1 = ''s1''), where there are two or four replicate samples for a given condition within an experiment. Neural constructs formed from NPCs, ECs, and PCs were used for analyzing variability between independent experiments, which included two replicate samples from experiment #1 and four replicate samples from experiment #2. The four replicates from experiment #2 also included two samples each from separate cryopreserved vials of NPCs, where each set of samples were seeded with the same ECs and PCs. (b–d) Immunofluorescence imaging illustrating endothelial cells (CD31, green), radial glial cells (GFAP, red), and nuclei (DAPI, blue) for neural constructs after 12 days of culture (ECs and primary pericytes were added on day 9). A zoom of the boxed region in (b) is shown in (c) for CD31 (green) and GFAP (red). The boxed region in (c) is show in (d) as single channels for CD31 and GFAP, and for the overlap between the two channels. Scale bars: (b) 100 μm; (c) 50 μm. (A color version of this figure is available in the online journal.)

N = 4 replicate samples, two samples from each independent experiment) (Figure 4(a)). Thus, multicellular neural constructs were characterized by highly correlated gene expression profiles for comparisons between similar samples, which was true for a wide range of conditions and time points.

Reproducibility between samples was further tested by determining the coefficient of variation (CV = S.D./Mean) for all expressed genes, which was defined as mean TPM ≥ 1 (Supplementary Table 4). Neural constructs formed under identical conditions within the same experiment were characterized by a mean CV ≤ 0.13 for all expressed genes (CV = 0.10 ± 0.09–0.13 ± 0.13; N = 4 replicate samples each for six separate comparisons; ≥13,838 genes were detected for all comparisons; Supplementary Table 4), while at least 98% of all expressed genes were characterized by CV ≤ 0.50 for each comparison. Neural constructs from two independent experiments were characterized by a mean CV for all expressed genes of 0.17 ± 0.13 on day 14 (N = 6 replicate samples from three cryopreserved vials of NPCs; 13,790 expressed genes) and 0.16 ± 0.11 on day 21 (N = 4 replicate samples, two from each experiment; 13,973 expressed genes), with more than 97% of all genes having CV ≤ 0.50 on both days (Figure 4(b), Supplementary Table 4). Thus, the mean variability in gene expression for sample replicates from independent

(a)

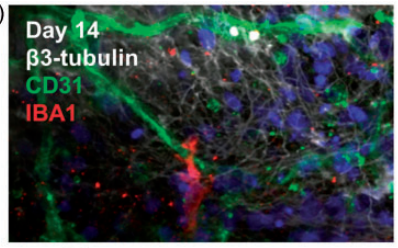

(b)

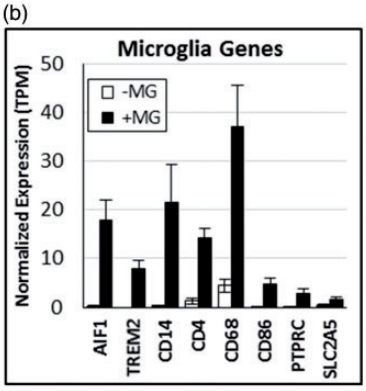

(c)

Term	Count
GO:0006955~immune response	94
GO:0006952~defense response	77
GO:0006954~inflammatory response	48
GO:0009611~response to wounding	55
GO:0002684~positive regulation of immune system process	33
GO:0045087~innate immune response	25
GO:0050778~positive regulation of immune response	24
GO:0042330~taxis	24
GO:0006935~chemotaxis	24
GO:0050865~regulation of cell activation	23

(d)

Day 14 ±MG		MSC (-MG)				PC (-MG)		MSC (+MG)				PC (+MG)	
	Sample	1	2	3	4	1	2	1	2	3	4	1	2
MSC (-MG)	1	1	0.99	0.99	0.99	0.99	0.99	0.98	0.98	0.98	0.98	0.98	0.98
	2	0.99	1	0.99	0.99	0.99	0.99	0.98	0.98	0.98	0.98	0.97	0.98
	3	0.99	0.99	1	0.99	0.99	0.99	0.98	0.98	0.98	0.98	0.97	0.98
	4	0.99	0.99	0.99	1	0.99	0.99	0.98	0.97	0.98	0.98	0.97	0.98
PC (-MG)	1	0.99	0.99	0.99	0.99	1	0.99	0.98	0.98	0.98	0.98	0.98	0.98
	2	0.99	0.99	0.99	0.99	0.99	1	0.98	0.98	0.98	0.98	0.98	0.98
MSC (+MG)	1	0.98	0.98	0.98	0.98	0.98	0.98	1	0.99	0.99	0.99	0.99	0.99
	2	0.98	0.98	0.98	0.97	0.98	0.98	0.99	1	0.99	0.99	0.99	0.99
	3	0.98	0.98	0.98	0.98	0.98	0.98	0.99	0.99	1	0.99	0.99	0.99
	4	0.98	0.98	0.98	0.98	0.98	0.98	0.99	0.99	0.99	1	0.99	0.99
PC (+MG)	1	0.98	0.97	0.97	0.97	0.98	0.98	0.99	0.99	0.99	0.99	1	0.99
	2	0.98	0.98	0.98	0.98	0.98	0.98	0.99	0.99	0.99	0.99	0.99	1

(e)

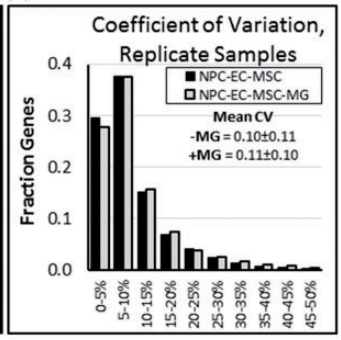

Figure 2 Characterization of sample reproducibility for multicomponent neural constructs formed with or without microglia. Neural constructs were formed with NPCs, ECs, MSCs or primary pericytes (PCs), and with or without microglia (MG). (a) Immunofluorescence imaging illustrating neurons (βIII-tubulin, white) and microglia (IBA1, red) for neural constructs formed with primary pericytes and microglia. (b) Mean normalized expression (TPM ± S.D.) of microglia genes for neural constructs formed with MSCs or primary pericytes and with or without microglia (N = 6 replicate samples from the same experiment; four MSC plus two PC samples; $p < 0.001$ for each of the genes shown). (c) The top 10 Gene Ontology terms for genes two-fold upregulated ($p < 0.001$) by neural constructs with microglia over samples without microglia. (d) Spearman's rank correlation coefficients for neural constructs formed with MSCs or primary pericytes and with or without microglia after 14 days of culture. Individual samples were formed during the same experiment. (e) The distribution of Coefficient of Variation (S.D. TPM/mean TPM) for neural constructs formed with MSCs and with or without microglia (N = 4 samples from the same experiment). (A color version of this figure is available in the online journal.)

experiments was ≤17%, including less than 10% variation between samples for many common neural genes (Figure 4(c)). These results demonstrate that model neural tissues with complex 3D organization can be produced from human pluripotent stem cells with high sample uniformity using standard culture techniques.

We next determined how NPCs from a distinct differentiation protocol would be influenced by culture on PEG hydrogels. We chose a recent protocol that uses a single neural differentiation medium (DF3S medium supplemented with N2, B27, and 100 ng/mL NOGGIN, see materials and methods section) to mimic human brain development for H1 ES cells cultured on Matrigel-coated tissue culture polystyrene (TCP) plates.[37] We compared RNA-Seq data from the previous study on TCP for the first 36 days of differentiation[37] to cells that were cultured on TCP for 14 days followed by PEG hydrogels for an additional 21 days. After 14 days of differentiation on TCP, cells were singularized and seeded on PEG-hydrogels at densities of 100,000 - 200,000 cells per well of 96-well round bottom plates and cultured for an additional 21 days, either in neural growth medium (N2B27 + 5 ng/mL FGF2) or in neural growth medium for seven days followed by DF3S medium (without added supplements or growth factors) for the remaining 14 days. Further, we compared PEG hydrogels with MMP-degradable crosslinks, such as for the ''multicomponent'' neural constructs described above, and non-degradable PEG-dithiol crosslinks.[22,23] The model neural tissues produced using this modified protocol were characterized by upregulated expression of genes within several neural development GO categories (Supplementary Table 3).

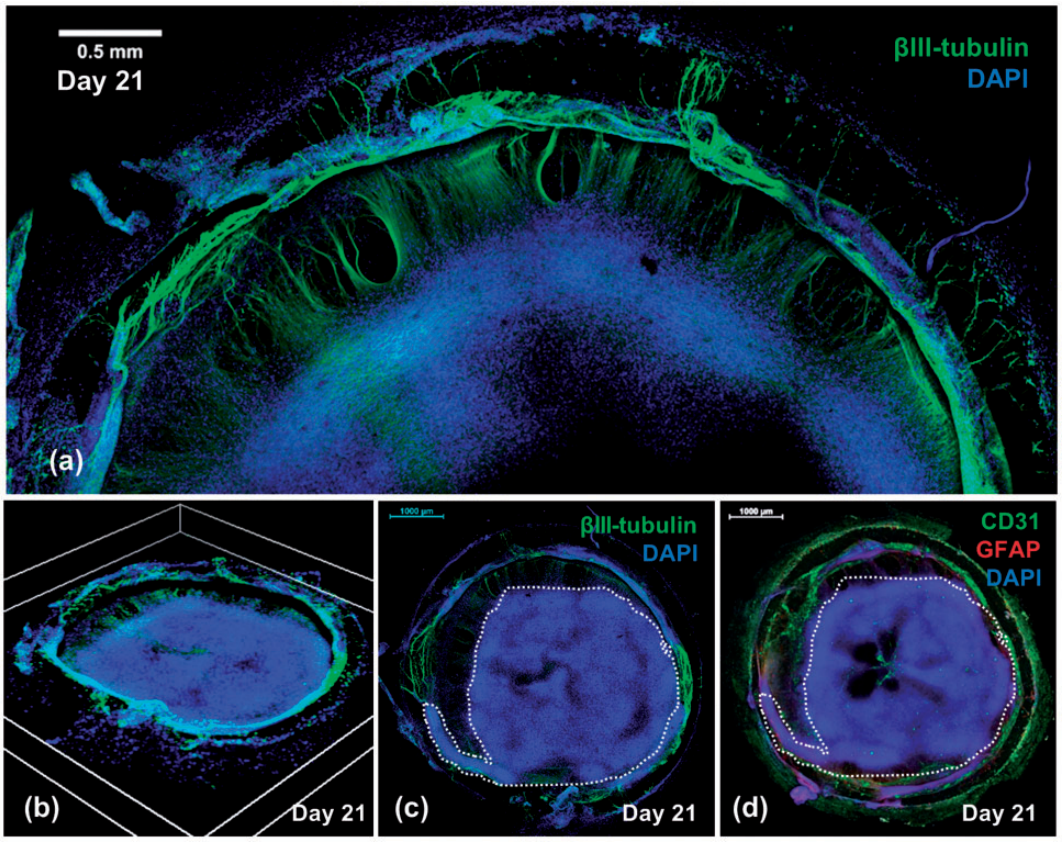

Figure 3 Multicomponent neural constructs after 21 days of culture. Neural tissue constructs formed with neural progenitor cells (NPCs), endothelial cells (ECs), mesenchymal stem cells (MSCs), and microglia precursor cells and cultured for 21 days. (a–c) Immunofluorescence imaging illustrating neurons (βIII-tubulin, green) and nuclei (DAPI, blue). The images in (a–c) are from the same sample, with (a) providing a higher resolution zoom and (b) illustrating a tilted z-stack top provide perspective on the thickness of the neural construct. (d) Immunofluorescence imaging illustrating endothelial cells (CD31, green), glial cells (GFAP, red), and nuclei (DAPI, blue). (c–d) The dotted line showing qualitative similarities in cellular organization; the outlined region illustrates dense nuclei staining for (c) and the same outline transposed onto (d). Scale bars: (a) 500 μm; (c,d) 1000 μm. (A color version of this figure is available in the online journal.)

The relevance of these in vitro neural samples to in vivo neural development was assessed by comparing correlation of RNA-Seq datasets to the human developmental biology resource (HDBR) expression dataset.[45] Spearman correlation coefficients were calculated using count data for genes with >0 reads that were detected in at least one of the three datasets, with results represented as heat maps to show relative correlations between neural samples and brain regions identified using the HDBR (Figure 5, Supplementary Figure 1). The TCP time course from RNA-Seq datasets that were previously published (GEO Series accession number GSE90053)[37] demonstrated that H1 ES cells differentiated down neural lineages became correlated with progressively later Carnegie stages over time, such as for forebrain development shown in Figure 5 (see Supplementary Figure 1 for other regions). The previous RNA-Seq datasets from our TCP neural culture time course were characterized by correlation to in vivo stages of human neural development that compared favorably to previous studies (Supplementary Figure 2)[41,42] using modifications of widely established neural differentiation and cerebral organoid procedures.[5,42]

Notably, when cells differentiated for 14 days on TCP were then transferred to PEG-hydrogels for an additional 21 days, samples were more highly correlated to in vivo Carnegie stages 20–23 than those cultured for the same amount of time on TCP alone (Figure 5, Supplementary Figure 1). Assuming that human ES cells at day 0 roughly correspond to embryonic day 15,[37] then samples cultured for 14 days on TCP and 21 additional days on PEG hydrogels transpose to embryonic day 50, which would be equivalent to Carnegie stages 19–20. Indeed, NPCs that were further differentiated on PEG-hydrogels using simple media formulations were characterized by higher correlation to later in vivo brain developmental stages than neural differentiation on TCP surfaces (Figure 5, Supplementary Figure 2).[37,41] The increase in correlation of in vitro samples cultured on PEG hydrogels to age-matched in vivo neural development compared to differentiation on TCP was observed for all media and hydrogel conditions tested, even when using the basal DF3S medium without neural supplements or growth factors for the final 14 days of culture.

"Single-component" neural constructs (Supplementary Table 5).[37] were characterized by lower sample uniformity than the multicomponent neural constructs described above (Supplementary Table 4), which was reflected in lower Spearman's correlation coefficients and higher CV

(a)

NPC-EC-PC			Day 14						Day 21				Day 47	
			Exp 1		Exp 2				Exp 1		Exp 2		Exp 1	
	Sample		1	2	1	2	1	2	1	2	1	2	1	2
Day 14	Exp 1	1	1	0.99	0.98	0.98	0.99	0.99	0.99	0.99	0.98	0.98	0.97	0.97
		2	0.99	1	0.98	0.98	0.99	0.99	0.99	0.99	0.98	0.98	0.97	0.97
	Exp 2	1	0.98	0.98	1	0.99	0.99	0.99	0.98	0.98	0.98	0.98	0.96	0.96
		2	0.98	0.98	0.99	1	0.99	0.99	0.98	0.98	0.98	0.98	0.97	0.97
		1	0.99	0.99	0.99	0.99	1	0.99	0.98	0.98	0.98	0.98	0.97	0.97
		2	0.99	0.99	0.99	0.99	0.99	1	0.98	0.98	0.98	0.98	0.97	0.97
Day 21	Exp 1	1	0.99	0.99	0.98	0.98	0.98	0.98	1	0.99	0.99	0.99	0.98	0.97
		2	0.99	0.99	0.98	0.98	0.98	0.98	0.99	1	0.99	0.99	0.98	0.97
	Exp 2	1	0.98	0.98	0.98	0.98	0.98	0.98	0.99	0.99	1	0.99	0.98	0.98
		2	0.98	0.98	0.98	0.98	0.98	0.98	0.99	0.99	0.99	1	0.98	0.98
Day 47	Exp 1	1	0.97	0.97	0.96	0.97	0.97	0.97	0.98	0.98	0.98	0.98	1	0.99
		2	0.97	0.97	0.96	0.97	0.97	0.97	0.97	0.97	0.98	0.98	0.99	1

(b)

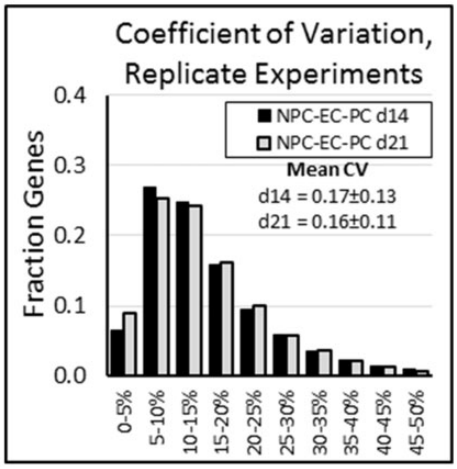

(c)

Mean TPM ± S.D., Day 21 (N = 4)		
Gene	TPM	CV
Nestin/NES	637.1±55.3	0.09
Vimentin/VIM	14548.9 ± 729	0.05
β3-tubulin/TUBB3	1458.7 ± 107.3	0.07
MAP2	2678.0 ± 29.4	0.11
VGLUT2/SLC17A6	73.3 ± 7.9	0.11
ACHE	49.2 ± 2.7	0.06
TH	119 ± 0.5	0.04
RBFOX3	10.1 ± 0.5	0.05
GAP43	1033.9 ± 147.8	0.14
SV2A	109.6 ± 7.2	0.07
Synaptophysin/SYP	102.8 ± 5.6	0.05
GAD1	17.0 ± 2.9	0.17
Calretinin/CALB2	216.5 ± 18.8	0.09
BRN2/POU3F2	113.2 ± 6.0	0.05
SATB1	44.2 ± 3.4	0.08
SOX2	287.8 ± 20.0	0.07
ETV1	10.9 ± 1.39	0.13
GFAP	127.1±28.2	0.22

Figure 4 Reproducibility of replicate multicomponent neural constructs up to 47 days of culture. Neural constructs were formed with NPCs, ECs, and primary pericytes (PCs) and cultured for up to 47 days. For day 14 samples, two separate experiments were conducted in which different cryopreserved vials of each cell type were used. For a second set of samples from experiment 2, two different cryopreserved vials of NPCs were used, but seeded with the same ECs and PCs on day 9. (a) Spearman's rank correlation coefficients demonstrate that replicate neural constructs are highly correlated for replicate samples and multiple experiments on days 14 and 21 and for replicate samples from the same experiment on day 47. (b) The distribution of coefficient of variation (S.D. TPM/mean TPM) for neural constructs from replicate experiments on day 14 (N = 6 replicate samples from two independent experiments) and day 21 (N = 4 replicate samples from two independent experiments). (c) Mean normalized expression and % standard deviation for select neuronal genes from day 21 neural constructs (N = 4 samples from two independent experiments).

values. The difference in variability could not be attributed to the support cells in the multicomponent neural constructs, since single-component samples formed using NPCs from the first protocol were also highly correlated (Supplementary Table 4: $\rho = 0.99$ for day 21 samples formed with 50,000 and 100,000 NPCs per well, ''NPCs only (control)''). There are several possible factors that might explain the reduced variability for the single-component neural constructs compared to the multicomponent neural constructs. For example, while the single-component neural constructs were cultured on PEG hydrogels formed in wells of round bottomed 96-well plates, the multicomponent neural constructs were cultured in 24-well transwell inserts. The hydrogel surface area is similar for the 96-well and 24-well transwell formats, but wells for 96-well plates have a much lower volume (~150 μL) than the 24-well transwell platform (~1.5 mL), which resulted in faster transition to yellow color after media exchange that would suggest dynamic differences in exposure to soluble factors. We also note that the differences in read depths for the multicomponent neural constructs (5.2×10^6–2.3×10^7 reads for all samples) was higher than single-component neural constructs (9.5×10^5–4.5×10^6 reads), which may also play a role in variability.

While variability was higher for the single-component compared to the multicomponent neural tissue models here, previous studies indicate that both platforms can be used to improve assays aimed towards toxicity screening and potency testing.[18,22] We previously demonstrated the value of the multicellular neural constructs for enhanced

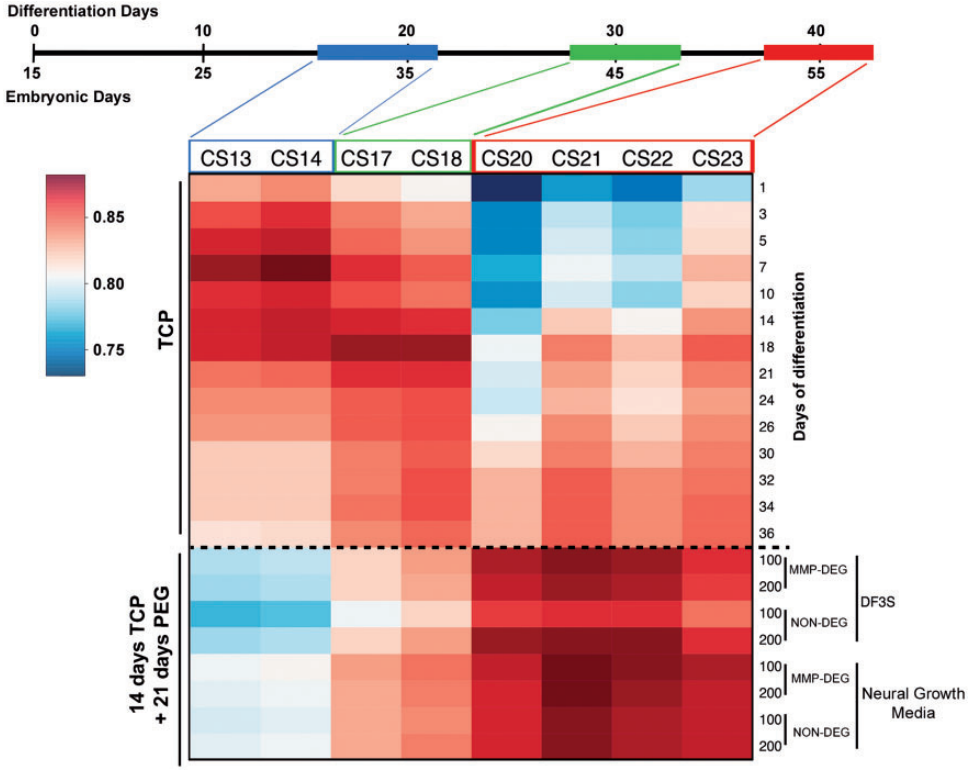

Figure 5 Comparison of neural differentiation on TCP and PEG hydrogels to in vivo human forebrain samples. RNA-seq of human H1 ES cells cultured in neural differentiation medium for 14 days on tissue culture polystyrene (TCP), followed by 21 days on PEG hydrogels, were analyzed for similarity to in vivo forebrain sections using Spearman correlations to the HDBR expression data set.[46] Cells cultured on hydrogels were either seeded on MMP-degradable (MMP-DEG) or non-degradable (NON-DEG) PEG hydrogels in DF3S medium or neural growth medium. For comparison, data from a previously reported time course of H1 ES cells differentiated entirely on TCP[37] were similarly correlated to HDBR. Spearman's rank correlations using genes with >0 reads in any dataset were included, and triplicate samples for hydrogel samples were averaged. Carnegie stages (CS) are shown corresponding to their observed day in vivo, along with the transposed day of differentiation, assuming that embryonic stem cells (day 0) correspond to human embryonic day 15. (A color version of this figure is available in the online journal.)

throughput neurotoxicity screening, achieving 90% accuracy in a blinded assessment of chemical compounds.[18] Additionally, human iPS cell-derived neural stem cells cultured on similar PEG hydrogels and the same 96-well format described here produced a functional neural phenotype that performed well in a botulinum neurotoxin potency testing assay.[22] Differentiation of the iPS cell-derived neural stem cells was enhanced on both MMP-degradable and non-degradable PEG hydrogels when compared to cells on TCP surfaces,[22] which led to improvements of the assay towards botulinum neurotoxin at earlier time points and sensitivity that was comparable to the in vivo mouse bioassay, which is the gold standard for potency testing.[59] While the role of culture media, hydrogel composition, and well format on neural maturation requires further investigation, our results demonstrate that human cellular models that mimic brain development can be produced with high uniformity using standard culture techniques rather than common organoid protocols such as suspension culture or encapsulation in Matrigel.

Authors' contributions: CB and MTS contributed equally to this article. CB, MTS, MPS, WLM, and JAT contributed to the design and interpretation of the study. CB, MTS, MPS, NEP, ZH, JZ, BKN, BEM, MDP, and JMB conducted experiments. CB, MTS, MPS, PJ, SS, and RS analyzed data. All authors reviewed the manuscript. CB, MTS, and MPS wrote the manuscript.

ACKNOWLEDGEMENTS

Funding for this work was provided by the Environmental Protection Agency (STAR grant no. 83573701) the U.S. Department of Health and Human Services National Institutes of Health (National Center for Advancing Translational Sciences #1UH2TR000506-01 and #1UH3TR 000506-01U.S., and National Heart, Lung, and Blood Institute #R01HL093282-01A1). CB was supported by a Canadian Institutes of Health Research Banting Postdoctoral Fellowship.

DECLARATION OF CONFLICTING INTERESTS

WLM is a founder and stockholder for Stem Pharm, Inc. and Tissue Regeneration Systems, Inc.

REFERENCES

1. Barker N, Huch M, Kujala P, van de Wetering M, Snippert HJ, van Es JH, Sato T, Stange DE, Begthel H, van den Born M, Danenberg E, van den Brink S, Korving J, Abo A, Peters PJ, Wright N, Poulsom R, Clevers H.

Lgr5(+ve) stem cells drive self-renewal in the stomach and build long-lived gastric units in vitro. *Cell Stem Cell* 2010;**6**:25–36
2. Spence JR, Mayhew CN, Rankin SA, Kuhar MF, Vallance JE, Tolle K, Hoskins EE, Kalinichenko VV, Wells SI, Zorn AM, Shroyer NF, Wells JM. Directed differentiation of human pluripotent stem cells into intestinal tissue in vitro. *Nature* 2011;**470**:105–U120
3. Takebe T, Sekine K, Enomura M, Koike H, Kimura M, Ogaeri T, Zhang RR, Ueno Y, Zheng YW, Koike N, Aoyama S, Adachi Y, Taniguchi H. Vascularized and functional human liver from an iPSC-derived organ bud transplant. *Nature* 2013;**499**:481–4
4. Xia Y, Nivet E, Sancho-Martinez I, Gallegos T, Suzuki K, Okamura D, Wu MZ, Dubova I, Esteban CR, Montserrat N, Campistol JM, Belmonte JCI. Directed differentiation of human pluripotent cells to ureteric bud kidney progenitor-like cells. *Nat Cell Biol* 2013;**15**:1507–15
5. Lancaster MA, Renner M, Martin CA, Wenzel D, Bicknell LS, Hurles ME, Homfray T, Penninger JM, Jackson AP, Knoblich JA. Cerebral organoids model human brain development and microcephaly. *Nature* 2013;**501**:373–9
6. Kadoshima T, Sakaguchi H, Nakano T, Soen M, Ando S, Eiraku M, Sasai Y. Self-organization of axial polarity, inside-out layer pattern, and species-specific progenitor dynamics in human ES cell-derived neocortex. *Proc Natl Acad Sci USA* 2013;**110**:20284–9
7. Mariani J, Simonini MV, Palejev D, Tomasini L, Coppola G, Szekely AM, Horvath TL, Vaccarino FM. Modeling human cortical development in vitro using induced pluripotent stem cells. *Proc Natl Acad Sci USA* 2012;**109**:12770–5
8. Eiraku M, Watanabe K, Matsuo-Takasaki M, Kawada M, Yonemura S, Matsumura M, Wataya T, Nishiyama A, Muguruma K, Sasail Y. Self-organized formation of polarized cortical tissues from ESCs and its active manipulation by extrinsic signals. *Cell Stem Cell* 2008;**3**:519–32
9. Passier R, Orlova V, Mummery C. Complex tissue and disease modeling using hiPSCs. *Cell Stem Cell* 2016;**18**:309–21
10. Low LA, Tagle DA. Organs-on-chips: progress, challenges, and future directions. *Exp Biol Med* 2017;**242**:1573–8
11. de Souza N. Organoid culture. *Nat Methods* 2017;**14**:35
12. Kelava I, Lancaster MA. Dishing out mini-brains: current progress and future prospects in brain organoid research. *Dev Biol* 2016;**420**:199–209
13. Hughes CS, Radan L, Betts D, Postovit LM, Lajoie GA. Proteomic analysis of extracellular matrices used in stem cell culture. *Proteomics* 2011;**11**:3983–91
14. Kleinman HK, McGarvey ML, Hassell JR, Star VL, Cannon FB, Laurie GW, Martin GR. Basement-membrane complexes with biological-activity. *Biochemistry* 1986;**25**:312–8
15. Orkin RW, Gehron P, McGoodwin EB, Martin GR, Valentine T, Swarm R. Murine tumor producing a matrix of basement membrane. *J Exp Med* 1977;**145**:204–20
16. Lindborg BA, Brekke JH, Vegoe AL, Ulrich CB, Haider KT, Subramaniam S, Venhuizen SL, Eide CR, Orchard PJ, Chen W, Wang Q, Pelaez F, Scott CM, Kokkoli E, Keirstead SA, Dutton JR, Tolar J, O'Brien TD. Rapid induction of cerebral organoids from human induced pluripotent stem cells using a chemically defined hydrogel and defined cell culture medium. *Stem Cells Transl Med* 2016;**5**:970–9
17. Cairns DM, Chwalek K, Moore YE, Kelley MR, Abbott RD, Moss S, Kaplan DL. Expandable and rapidly differentiating human induced neural stem cell lines for multiple tissue engineering applications. *Stem Cell Reports* 2016;**7**:557–70
18. Schwartz MP, Hou Z, Propson NE, Zhang J, Engstrom CJ, Costa VS, Jiang P, Nguyen BK, Bolin JM, Daly W, Wang Y, Stewart R, Page CD, Murphy WL, Thomson JA. Human pluripotent stem cell-derived neural constructs for predicting neural toxicity. *Proc Natl Acad Sci USA* 2015;**112**:12516–21
19. Meinhardt A, Eberle D, Tazaki A, Ranga A, Niesche M, Wilsch-Bräuninger M, Stec A, Schackert G, Lutolf M, Tanaka EM. 3D reconstitution of the patterned neural tube from embryonic stem cells. *Stem Cell Reports* 2014;**3**:987–999
20. Fairbanks BD, Schwartz MP, Halevi AE, Nuttelman CR, Bowman CN, Anseth KS. A versatile synthetic extracellular matrix mimic via thiol-norbornene photopolymerization. *Adv Mater* 2009;**21**:5005–10
21. McKinnon DD, Kloxin AM, Anseth KS. Synthetic hydrogel platform for three-dimensional culture of embryonic stem cell-derived motor neurons. *Biomater Sci* 2013;**1**:460–9
22. Pellett S, Schwartz MP, Tepp WH, Josephson R, Scherf JM, Pier CL, Thomson JA, Murphy WL, Johnson EA. Human induced pluripotent stem cell derived neuronal cells cultured on chemically-defined hydrogels for sensitive in vitro detection of botulinum neurotoxin. *Sci Rep* 2015;**5**:14566
23. Musah S, Wrighton PJ, Zaltsman Y, Zhong X, Zorn S, Parlato MB, Hsiao C, Palecek SP, Chang Q, Murphy WL, Kiessling LL. Substratum-induced differentiation of human pluripotent stem cells reveals the coactivator YAP is a potent regulator of neuronal specification. *Proc Natl Acad Sci* 2014;**111**:13805–10
24. Tarus D, Hamard L, Caraguel F, Wion D, Szarpak-Jankowska A, van der Sanden B, Auzély-Velty R. Design of hyaluronic acid hydrogels to promote neurite outgrowth in three dimensions. *ACS Appl Mater Interfaces* 2016;**8**:25051–9
25. Gramlich WM, Kim IL, Burdick JA. Synthesis and orthogonal photopatterning of hyaluronic acid hydrogels with thiol-norbornene chemistry. *Biomaterials* 2013;**34**:9803–11
26. Hynes WF, Doty NJ, Zarembinski TI, Schwartz MP, Toepke MW, Murphy WL, Atzet SK, Clark R, Melendez JA, Cady NC. Micropatterning of 3D microenvironments for living biosensor applications. *Biosensors* 2014;**4**:28–44
27. Munoz Z, Shih H, Lin CC. Gelatin hydrogels formed by orthogonal thiol-norbornene photochemistry for cell encapsulation. *Biomater Sci* 2014;**2**:1063–72
28. Lin C-C, Ki CS, Shih H. Thiol–norbornene photoclick hydrogels for tissue engineering applications. *J Appl Polym Sci* 2015;**132**:41563
29. Hughes CS, Postovit LM, Lajoie GA. Matrigel: a complex protein mixture required for optimal growth of cell culture. *Proteomics* 2010;**10**:1886–90
30. Nagase H, Fields GB. Human matrix metalloproteinase specificity studies using collagen sequence-based synthetic peptides. *Biopolymers* 1996;**40**:399–416
31. Ruoslahti E. RGD and other recognition sequences for integrins. *Annu Rev Cell Dev Biol* 1996;**12**:697–715
32. Pierschbacher MD, Ruoslahti E. Cell attachment activity of fibronectin can be duplicated by small synthetic fragments of the molecule. *Nature* 1984;**309**:30–3
33. Schwartz MP, Rogers RE, Singh SP, Lee JY, Loveland SG, Koepsel JT, Witze ES, Montanez-Sauri SI, Sung KE, Tokuda EY, Sharma Y, Everhart LM, Nguyen EH, Zaman MH, Beebe DJ, Ahn NG, Murphy WL, Anseth KS. A quantitative comparison of human HT-1080 fibrosarcoma cells and primary human dermal fibroblasts identifies a 3D migration mechanism with properties unique to the transformed phenotype. *PLoS One* 2013;**8**:e81689
34. Anderson SB, Lin CC, Kuntzler DV, Anseth KS. The performance of human mesenchymal stem cells encapsulated in cell-degradable polymer-peptide hydrogels. *Biomaterials* 2011;**32**:3564–74
35. Hou Z, Zhang J, Schwartz MP, Stewart R, Page CD, Murphy WL, Thomson JA. A human pluripotent stem cell platform for assessing developmental neural toxicity screening. *Stem Cell Res Ther* 2013;**4**(Suppl 1): S12
36. Chen GK, Gulbranson DR, Hou ZG, Bolin JM, Ruotti V, Probasco MD, Smuga-Otto K, Howden SE, Diol NR, Propson NE, Wagner R, Lee GO, Antosiewicz-Bourget J, Teng JMC, Thomson JA. Chemically defined conditions for human iPSC derivation and culture. *Nat Methods* 2011;**8**:424–9
37. Barry C, Schmitz MT, Jiang P, Schwartz MP, Duffin BM, Swanson S, Bacher R, Bolin JM, Elwell AL, McIntosh BE, Stewart R, Thomson JA. Species-specific developmental timing is maintained by pluripotent stem cells ex utero. *Dev Biol* 2017;**423**:101–10
38. Schneider CA, Rasband WS, Eliceiri KW. NIH Image to ImageJ: 25 years of image analysis. *Nat Meth* 2012;**9**:671–5
39. Barrett T, Wilhite SE, Ledoux P, Evangelista C, Kim IF, Tomashevsky M, Marshall KA, Phillippy KH, Sherman PM, Holko M, Yefanov A, Lee H, Zhang N, Robertson CL, Serova N, Davis S,

Soboleva A. NCBI GEO: archive for functional genomics data sets – update. *Nucleic Acids Res* 2013;**41**:D991–5
40. Edgar R, Domrachev M, Lash AE. Gene expression omnibus: NCBI gene expression and hybridization array data repository. *Nucleic Acids Res* 2002;**30**:207–10
41. van de Leemput J, Boles NC, Kiehl TR, Corneo B, Lederman P, Menon V, Lee C, Martinez RA, Levi BP, Thompson CL, Yao S, Kaykas A, Temple S, Fasano CA. CORTECON: a temporal transcriptome analysis of In Vitro human cerebral cortex development from human embryonic stem cells. *Neuron* 2014;**83**:51–68
42. Dang J, Tiwari SK, Lichinchi G, Qin Y, Patil VS, Eroshkin AM, Rana TM. Zika virus depletes neural progenitors in human cerebral organoids through activation of the innate immune receptor TLR3. *Cell Stem Cell* 2016;**19**:258–65
43. Langmead B, Trapnell C, Pop M, Salzberg S. Ultrafast and memory-efficient alignment of short DNA sequences to the human genome. *Genome Biol* 2009;**10**:R25
44. Li B, Dewey CN. RSEM: accurate transcript quantification from RNA-Seq data with or without a reference genome. *BMC Bioinformatics* 2011;**12**:323
45. Lindsay SJ, Xu Y, Lisgo SN, Harkin LF, Copp AJ, Gerrelli D, Clowry GJ, Talbot A, Keogh MJ, Coxhead J. HDBR expression: a unique resource for global and individual gene expression studies during early human brain development. *Front Neuroanat* 2016;**10**:86
46. Huang DW, Sherman BT, Lempicki RA. Systematic and integrative analysis of large gene lists using DAVID bioinformatics resources. *Nat Protocols* 2008;**4**:44–57
47. Ashburner M, Ball CA, Blake JA, Botstein D, Butler H, Cherry JM, Davis AP, Dolinski K, Dwight SS, Eppig JT, Harris MA, Hill DP, Issel-Tarver L, Kasarskis A, Lewis S, Matese JC, Richardson JE, Ringwald M, Rubin GM, Sherlock G, Gene Ontology C. Gene Ontology: tool for the unification of biology. *Nature Genet* 2000;**25**:25–9
48. Bystron I, Blakemore C, Rakic P. Development of the human cerebral cortex: Boulder Committee revisited. *Nat Rev Neurosci* 2008;**9**:110–22
49. Bystron I, Rakic P, Molnar Z, Blakemore C. The first neurons of the human cerebral cortex. *Nat Neurosci* 2006;**9**:880–6
50. Zecevic N. Specific characteristic of radial glia in the human fetal telencephalon. *Glia* 2004;**48**:27–35
51. Meyer G, Schaaps JP, Moreau L, Goffinet AM. Embryonic and early fetal development of the human neocortex. *J Neurosci* 2000;**20**:1858–68
52. Zecevic N, Milosevic A, Rakic S, Marín-Padilla M. Early development and composition of the human primordial plexiform layer: an immunohistochemical study. *J Comp Neurol* 1999;**412**:241–54
53. Marin-Padilla M. The human brain intracerebral microvascular system: development and structure. *Front Neuroanat* 2012;**6**:38
54. James JM, Mukouyama Y-s. Neuronal action on the developing blood vessel pattern. *Semin Cell Dev Biol* 2011;**22**:1019–27
55. Kettenmann H, Hanisch UK, Noda M, Verkhratsky A. Physiology of microglia. *Physiol Rev* 2011;**91**:461–553
56. Ginhoux F, Greter M, Leboeuf M, Nandi S, See P, Gokhan S, Mehler MF, Conway SJ, Ng LG, Stanley ER, Samokhvalov IM, Merad M. Fate mapping analysis reveals that adult microglia derive from primitive macrophages. *Science* 2010;**330**:841–5
57. Monier A, Adle-Biassette H, Delezoide AL, Evrard P, Gressens P, Verney C. Entry and distribution of microglial cells in human embryonic and fetal cerebral cortex. *J Neuropathol Exp Neurol* 2007;**66**:372–82
58. Lancaster MA, Knoblich JA. Organogenesis in a dish: modeling development and disease using organoid technologies. *Science* 2014;**345**:1247125
59. Pellett S. Progress in cell based assays for botulinum neurotoxin detection. In: Rummel A, Binz T (eds). *Botulinum neurotoxins*. Vol. 364, Berlin: Springer-Verlag Berlin, 2013, pp. 257–285